Modal Power Flow Analysis of a Damaged Composite Plate

Waion WONG* Yanlung CHEUNG* and Li CHENG*
*Department of Mechanical Engineering
The Hong Kong Polytechnic University, Hong Kong SAR, China
E-mail: mmwowong@polyu.edu.hk

Abstract
Variation of the modal reactive power distribution of a damaged composite plate is modeled and analyzed both analytically and numerically. Large variation of local reactive power flow in or around the damage region of a plate under resonant vibration is related to the change of strain and kinetic energies in the damage region. Feasibility of damage identification based on the detection of this local variation of modal reactive power flow in a structure is studied. Compared with the damage identification techniques based on the determination of the active power flow in a damaged plate, the proposed method only requires data of a vibration mode shape of the structure and it is easier to apply in practice. Modal power flow of an orthotropic plate with a region of reduced stiffness in the plate is analyzed. Numerical tests show that the proposed method is effective for detection of the damage and the modal power flow is more sensitive to the change of plate stiffness than the strain mode shape in the test case.

Key words: Power flow, Damage, Composite

1. Introduction

Detection of damage occurring in structures is an important topic in mechanical and structural engineering applications [1-3]. Identification of damage location is crucial for damage repair and control and there have been many techniques developed for damage identification and location in recent years [4-7]. One relatively new technique is based on the study of power flow or structural intensity (SI) in a vibrating structure. There are in general active and reactive powers presented in a vibrating structure. Active power is defined as the product of a generalized force with the in-phase component of a generalized velocity, where the velocity is in the same direction as the force. Forces and velocities in a vibrating structure will be exactly 90 degrees out of phase if no damping and no energy dissipation such as sound radiation in the system is assumed. The product of the corresponding force and velocity terms is called the reactive power which represents the amount of energy stored in the structure [8].

Li *et al.*[9] proposed the diagnosis of flaws in damaged beam structures using vibrational power flow. Khun *et al.*[10] showed that loosened bolt joints in plate assembly could be identified from the power flow pattern in the plates. Lee *et al.* [11] calculated the diversion of energy flow near crack tips of a vibrating plate using structural intensity technique. They showed that the presence of a crack can be identified by the changes of the directions of SI vectors near the crack. In all these reported methods, however, the forced vibration data of an excited structure were required. Accordingly, it was the active power flow which was used for damage identification. There is no report found in the literature about the use of reactive power flow in a plate for damage identification.

The aim of this paper is to study the power flow and energy distribution of a vibration mode of a damaged composite plate. The power flow is shown to be of reactive nature in this case, and referred to as the modal power flow in the following. The outline of this paper is as follows. In section 2, the modal power flow analysis of the damaged plate is performed, and the relation between the modal power flow and the modal energy distribution in the plate is derived. The modal power flow is proposed to locate damage sites in plate-like structures. In section 3, some numerical simulations are demonstrated to analyze the identification capability of the proposed damage indicator. Finally, conclusions are drawn.

2. Modal Power flow analysis of a damaged plate

From plate theory, the equation of motion of a thin vibrating orthotropic plate may be written as

$$\left(D_x \frac{\partial^4 w}{\partial x^4} + 2H \frac{\partial^4 w}{\partial x^2 \partial y^2} + D_y \frac{\partial^4 w}{\partial y^4}\right) + \rho h \frac{\partial^2 w}{\partial t^2} = 0 \tag{1}$$

(1)

where $D_x = \dfrac{E_x h^3}{12(1-\nu_x \nu_y)}$, $D_y = \dfrac{E_y h^3}{12(1-\nu_y \nu_x)}$, $H = \nu_x D_y + 2D_{xy}$ and $D_{xy} = Gh^3/12$, in which E_x and E_y are the moduli of elasticity in the x and y directions respectively, G_{xy} is the shear modulus, ν_x and ν_y are Poisson ratios, h is the thickness of the plate, and ρ is the material density. D_x and D_y are called the flexural rigidities and D_{xy} is the torsional rigidity of the plate, $2H$ is called the effective torsional rigidity of the orthotropic plate, and w is the transverse deflection in the z-direction.

Assuming the plate has a harmonic motion of frequency ω, its displacement may be written as

$$w(x, y; t) = W(x, y) \sin \omega t \tag{2}$$

where $W(x, y)$ is the vibration amplitude of the plate.
The strain distributions of the plate may be written as

$$\Psi_x(x,y) = \frac{\partial^2 W(x,y)}{\partial x^2}, \quad \Psi_y(x,y) = \frac{\partial^2 W(x,y)}{\partial y^2}, \quad \Psi_{xy}(x,y) = \frac{\partial^2 W(x,y)}{\partial x \partial y}. \tag{3}$$

The instantaneous power flow at point (x, y) may be written as [12]

$$\vec{P}(x, y; t) = P_x(x, y; t)\vec{i} + P_y(x, y; t)\vec{j} \tag{4}$$

where

$$P_x(x,y;t) = \frac{\partial}{\partial x}\left(D_x \frac{\partial^2 w}{\partial x^2} + H \frac{\partial^2 w}{\partial y^2}\right)\dot{w} - D_x\left(\frac{\partial^2 w}{\partial x^2} + \nu_y \frac{\partial^2 w}{\partial y^2}\right)\frac{\partial \dot{w}}{\partial x} - 2D_{xy}\frac{\partial^2 w}{\partial x \partial y}\frac{\partial \dot{w}}{\partial y}, \text{ and} \tag{5}$$

$$P_y(x,y;t) = \frac{\partial}{\partial y}\left(D_y \frac{\partial^2 w}{\partial y^2} + H \frac{\partial^2 w}{\partial x^2}\right)\dot{w} - D_y\left(\frac{\partial^2 w}{\partial y^2} + \nu_x \frac{\partial^2 w}{\partial x^2}\right)\frac{\partial \dot{w}}{\partial y} - 2D_{xy}\frac{\partial^2 w}{\partial y \partial x}\frac{\partial \dot{w}}{\partial x}. \tag{6}$$

2.1. Relationship between power flow and energy distributions of a vibrating plate

Equation (5) may be rewritten using equations (2) and (3) as

$$\begin{aligned} P_x(x,y;t) &= \frac{\partial}{\partial x}\left(D_x \frac{\partial^2 w}{\partial x^2} + H \frac{\partial^2 w}{\partial y^2}\right)\dot{w} - D_x\left(\frac{\partial^2 w}{\partial x^2} + \nu_y \frac{\partial^2 w}{\partial y^2}\right)\frac{\partial \dot{w}}{\partial x} - 2D_{xy}\frac{\partial^2 w}{\partial x \partial y}\frac{\partial \dot{w}}{\partial y} \\ &= \frac{1}{2}\omega\left[\frac{\partial(D_x \Psi_x + H\Psi_y)}{\partial x} W - D_x(\Psi_x + \nu_y \Psi_y)\frac{\partial W}{\partial x} - 2D_{xy}\Psi_{xy}\frac{\partial W}{\partial y}\right]\cdot \sin 2\omega t \\ &= P_{x\_\max} \sin 2\omega t \end{aligned} \tag{7a}$$

$$\text{where } P_{x\_\max} = \frac{1}{2}\omega\left[\frac{\partial(D_x\Psi_x + H\Psi_y)}{\partial x}W - D_x(\Psi_x + \nu_y\Psi_y)\frac{\partial W}{\partial x} - 2D_{xy}\Psi_{xy}\frac{\partial W}{\partial y}\right] \tag{7b}$$

Equation (6) may be rewritten using equations (2) and (3) as

$$\begin{aligned} P_y(x,y;t) &= \frac{\partial}{\partial y}\left(D_y\frac{\partial^2 w}{\partial y^2} + H\frac{\partial^2 w}{\partial x^2}\right)\dot{w} - D_y(\frac{\partial^2 w}{\partial y^2} + \nu_x\frac{\partial^2 w}{\partial x^2})\frac{\partial \dot{w}}{\partial y} - 2D_{xy}\frac{\partial^2 w}{\partial y\partial x}\frac{\partial \dot{w}}{\partial x} \\ &= \frac{1}{2}\omega\left[\frac{\partial(D_y\Psi_y + H\Psi_x)}{\partial y}W - D_y(\Psi_y + \nu_x\Psi_x)\frac{\partial W}{\partial y} - 2D_{xy}\Psi_{xy}\frac{\partial W}{\partial x}\right]\cdot\sin 2\omega t \\ &= P_{y\_\max}\sin 2\omega t \end{aligned} \tag{8a}$$

$$\text{where } P_{y\_\max} = \frac{1}{2}\omega\left[\frac{\partial(D_y\Psi_y + H\Psi_x)}{\partial y}W - D_y(\Psi_y + \nu_x\Psi_x)\frac{\partial W}{\partial y} - 2D_{xy}\Psi_{xy}\frac{\partial W}{\partial x}\right] \tag{8b}$$

The power gradients may be written as

$$\begin{aligned} \frac{\partial P_x}{\partial x} = \frac{1}{2}\omega\Bigg[&\frac{\partial^2(D_x\Psi_x + H\Psi_y)}{\partial x^2}W + \frac{\partial(D_x\Psi_x + H\Psi_y)}{\partial x}\frac{\partial W}{\partial x} - D_x(\frac{\partial \Psi_x}{\partial x} + \nu_y\frac{\partial \Psi_y}{\partial x})\frac{\partial W}{\partial x} \\ &-D_x(\Psi_x + \nu_y\Psi_y)\Psi_x - 2D_{xy}\Psi_{xy}\Psi_{xy} - 2D_{xy}\frac{\partial \Psi_{xy}}{\partial x}\frac{\partial W}{\partial y}\Bigg]\sin 2\omega t \end{aligned} \tag{9}$$

and

$$\begin{aligned} \frac{\partial P_y}{\partial y} = \frac{1}{2}\omega\Bigg[&\frac{\partial^2(D_y\Psi_y + H\Psi_x)}{\partial y^2}W + \frac{\partial(D_y\Psi_y + H\Psi_x)}{\partial y}\frac{\partial W}{\partial y} - D_y(\frac{\partial \Psi_y}{\partial y} + \nu_x\frac{\partial \Psi_x}{\partial y})\frac{\partial W}{\partial y} \\ &-D_y(\Psi_y + \nu_x\Psi_x)\Psi_y - 2D_{xy}\Psi_{xy}\Psi_{xy} - 2D_{xy}\frac{\partial \Psi_{xy}}{\partial y}\frac{\partial W}{\partial x}\Bigg]\sin 2\omega t \end{aligned} \tag{10}$$

The power flow $\bar{P}(x,y;t)$ can be related to the instantaneous energy stored in the plate in the following. The distribution of the instantaneous kinetic energy of the plate may be written as

$$\begin{aligned} T &= \frac{1}{2}\rho h\omega^2 W^2\cos^2\omega t \\ &= T_{\max}\cos^2\omega t \end{aligned} \tag{11}$$

$$\text{where } T_{\max} = \frac{1}{2}\rho h\omega^2 W^2. \tag{12}$$

The distribution of the instantaneous strain energy of the plate may be written as

$$\begin{aligned} U &= \frac{1}{2}\omega\left[D_x{\Psi_x}^2 + D_y{\Psi_y}^2 + 2\nu_x D_y\Psi_x\Psi_y + 4D_{xy}\left(\Psi_{xy}\right)^2\right]\sin^2\omega t \\ &= U_{\max}\sin^2\omega t \end{aligned} \tag{13}$$

$$\text{where } U_{\max} = \frac{1}{2}\omega\left[D_x{\Psi_x}^2 + D_y{\Psi_y}^2 + 2\nu_x D_y\Psi_x\Psi_y + 4D_{xy}\left(\Psi_{xy}\right)^2\right]. \tag{14}$$

The instantaneous energy and distributions in the plate are written respectively as

$$\begin{aligned} E &= T_{\max}\cos^2\omega t + U_{\max}\sin^2\omega t \\ &= \tfrac{1}{2}\left(T_{\max} + U_{\max}\right) + \tfrac{1}{2}\left(T_{\max} - U_{\max}\right)\cos 2\omega t, \text{ and} \end{aligned} \tag{15}$$

$$\frac{\partial E}{\partial t} = \omega\left(T_{\max} - U_{\max}\right)\sin 2\omega t. \tag{16}$$

Using equations (9) and (10), the sum of the power flow gradients can be written as

$$\frac{\partial P_x}{\partial x} + \frac{\partial P_y}{\partial y} = \frac{1}{2}\omega\left[\frac{\partial^2(D_x\Psi_x + H\Psi_y)}{\partial x^2}W + \frac{\partial^2(D_y\Psi_y + H\Psi_x)}{\partial y^2}W\right.$$

$$-D_x\Psi_x^{\ 2} - D_y\Psi_y^{\ 2} - 2\nu_x D_y\Psi_x\Psi_y - 4D_{xy}\left(\Psi_{xy}\right)^2\Big]\sin 2\omega t \tag{17}$$

Equation (1) may be rewritten using (2) as

$$D_x\frac{\partial^4 W}{\partial x^4} + 2H\left(\frac{\partial^2 W}{\partial x^2}\frac{\partial^2 W}{\partial y^2}\right) + D_y\frac{\partial^4 W}{\partial y^4} = \rho h\omega^2 W \tag{18}$$

Equation (17) can be rewritten using equation (18) as

$$\frac{\partial P_x}{\partial x} + \frac{\partial P_y}{\partial y} = \frac{1}{2}\omega\left\{\rho h\omega^2 W^2 - \left[D_x\Psi_x^{\ 2} + D_y\Psi_y^{\ 2} + 2\nu_x D_y\Psi_x\Psi_y + 4D_{xy}\left(\Psi_{xy}\right)^2\right]\right\}\sin 2\omega t \tag{19}$$

Using equations (12), (14) and (16), the instantaneous energy balance at a point (x,y) of the plate may be written as

$$\frac{\partial P_x}{\partial x} + \frac{\partial P_y}{\partial y} = \frac{\partial E}{\partial t} \tag{20}$$

The net power flow out of a region $x_1 \le x \le x_2$ and $y_1 \le y \le y_2$ can be obtained by integrating the above equation along x direction from x_1 to x_2 and along y direction from y_1 to y_2 and the result may be written as

$$\int_{y_1}^{y_2}\left[P_x(x_2) - P_x(x_1)\right]dy + \int_{x_1}^{x_2}\left[P_y(y_2) - P_y(y_1)\right]dx = \omega\int_{y_1}^{y_2}\int_{x_1}^{x_2}\left(T_{\max} - U_{\max}\right)dx\,dy\sin 2\omega t \tag{21}$$

This energy flow and balance in a region of the plate is illustrated in Fig. 1.

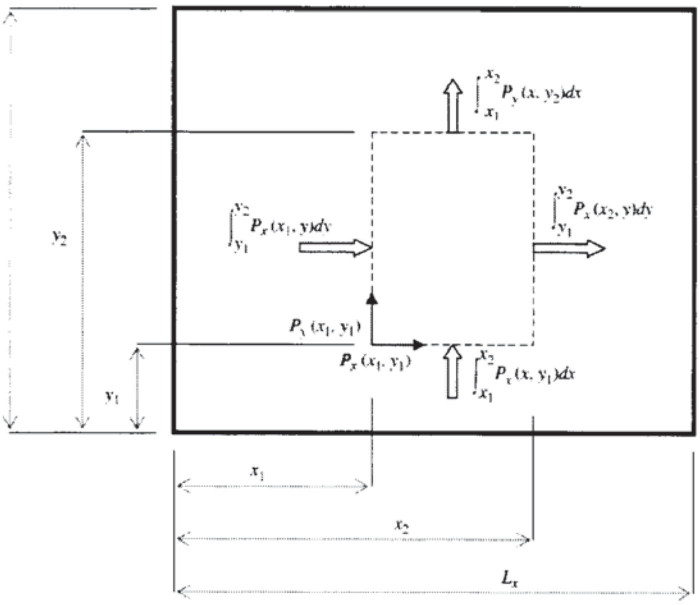

Fig. 1. Illustration of the power flow in and out of a region (as shown by the hollow arrows) in a vibrating plate.

Using equations (7), (8), (16) and (20), we may write

$$\frac{\partial P_{x\_\max}}{\partial x} + \frac{\partial P_{y\_\max}}{\partial y} = \omega\left(T_{\max} - U_{\max}\right) \tag{22}$$

Equation (22) shows that the sum of power flow gradients is proportional to the Lagrangian density $\left(T_{\max} - U_{\max}\right)$ of the plate.

2.2. Modal power flow of a plate

Since damping is neglected in the present analysis, the force and moment terms has no in-phase component of the corresponding velocity terms in the calculation of the power flow of a vibration mode of the plate. Therefore, the power flow of a vibration mode of the plate is the reactive power associated with that particular mode and it is termed as the modal power flow in the following analysis.

Using equations (4), (5) and (6), the reactive power flow at the mn^{th} mode where m, n = 1, 2, 3..., may be defined as

$$\vec{P}_{mn}(x,y;t) = P_{mn\_x}(x,y)\sin 2\omega_{mn}t\,\vec{i} + P_{mn\_y}(x,y)\sin 2\omega_{mn}t\,\vec{j} \tag{23}$$

where

$$P_{mn\_x}(x,y) = \omega_{mn}\left[\left(D_x\frac{\partial^3 W_{mn}}{\partial x^3} + H\frac{\partial^3 W_{mn}}{\partial y^3}\right)W_{mn} - D_x\left(\frac{\partial^2 W_{mn}}{\partial x^2} + \nu\frac{\partial^2 W_{mn}}{\partial y^2}\right)\frac{\partial W_{mn}}{\partial x} - 2D_{xy}\frac{\partial^2 W_{mn}}{\partial x\partial y}\frac{\partial W_{mn}}{\partial y}\right] \tag{24}$$

and

$$P_{mn\_y}(x,y) = \omega_{mn}\left[\left(D_y\frac{\partial^3 W_{mn}}{\partial y^3} + H\frac{\partial^3 W_{mn}}{\partial x^3}\right)W_{mn} - D_y\left(\frac{\partial^2 W_{mn}}{\partial y^2} + \nu\frac{\partial^2 W_{mn}}{\partial x^2}\right)\frac{\partial W_{mn}}{\partial y} - 2D_{xy}\frac{\partial^2 W_{mn}}{\partial y\partial x}\frac{\partial W_{mn}}{\partial x}\right] \tag{25}$$

where ω_{mn} and W_{mn} are the natural frequency and mode shape of the mn^{th} vibration mode of the plate, respectively. From equation (20), the modal power flow can be related to the modal energy distribution of the plate as

$$\frac{\partial P_{mn\_x}}{\partial x} + \frac{\partial P_{mn\_y}}{\partial y} = \omega_{mn}\left(T_{mn\_\max} - U_{mn\_\max}\right) \tag{26}$$

where $T_{mn\_\max} = \frac{1}{2}\rho h \omega_{mn}{}^2 W_{mn}{}^2$, and (27)

$$U_{mn\_\max} = \frac{1}{2}\omega_{mn}\left[D_x\left(\frac{\partial^2 W_{mn}}{\partial x^2}\right)^2 + D_y\left(\frac{\partial^2 W_{mn}}{\partial y^2}\right)^2 + 2\nu_x D_y\frac{\partial^2 W_{mn}}{\partial x^2}\frac{\partial^2 W_{mn}}{\partial y^2} + 4D_{xy}\left(\frac{\partial^2 W_{mn}}{\partial x\partial y}\right)^2\right] \tag{28}$$

2.3. Damage identification from the modal power flow of a plate

This part deals with the damage identification in a plate using the information about modal power flow. The basic concept is that a localized loss of stiffness will produce a curvature increase at the same location [2]. If no change of mass in the damage region is assumed, this local change of curvature would induce a local change of bending strains [5] and strain energy distribution [6] around the damage region resulting in the change of the gradients of power flow around the region as depicted by equation (26). This change of modal power flow may be more sensitive to the damage as it is a higher order derivative of the mode shape than the strain distribution of the plate [13].

The modal power flow vector field may be rewritten as

$$\frac{\vec{P}_{mn}(x,y;t)}{\omega_{mn}} = \left[\tilde{P}_{mn\_x}(x,y)\,\vec{i} + \tilde{P}_{mn\_y}(x,y)\,\vec{j}\right]\sin 2\omega_{mn}t \tag{29}$$

The vector field $\vec{P}_{mn}(x,y)/\omega_{mn} = \tilde{P}_{mn\_x}\,\vec{i} + \tilde{P}_{mn\_y}\,\vec{j}$ is proposed to be used for damage identification and location in plate-like structures. The advantage of using this term is that both the modal power flow components $\tilde{P}_{mn\_x}$ and $\tilde{P}_{mn\_y}$ can be derived by the mode shape data which can be obtained with a standard modal testing procedure [14].

3. Simulation analyses

Modal power flow an orthotropic plate with a region of reduced stiffness in the plate is calculated according to the theory in Section 2. The vibration modes and hence the modal power flow of a simply-supported rectangular plate with the damage are calculated with a self-developed *Matlab* program based on the Rayleigh-Ritz method [5,15]. Changes of modal energy distributions and power flow due to the damage in a plate are compared and discussed in the following sections. Modal power flow and modal energy distributions are calculated according to equations (24), (25), (27) and (28).

3.1 Simulation of the modal power flow in a composite plate

A simply-supported orthotropic square plate of size 1 x 1 x 0.01 m^3 is used in the simulation. It is assumed that $E_x/E_y = 10$ and $v_x = 0.25$. In applying the Rayleigh-Ritz method, the r^{th} mode shape function of the plate is expressed in a series written as [5,15]

$$W_r(x,y) = \sum_{i=1}^{p}\sum_{j=1}^{q} c_{r,ij} \cdot \varphi_i(x) \cdot \eta_j(y) \tag{30}$$

where $\varphi_i(x)$ and $\eta_j(y)$ are appropriate admissible functions, $c_{r,ij}$ the unknown coefficients. $p = q = 20$ is applied in the calculation of the mode shape functions.

Contour plots of the calculated mode shape functions and modal energy distributions are generated and displayed by using the CONTOUR function in Matlab. Fig. 2(a) shows the contours of the vibration mode W_{11} of the plate. Modal energy distributions of the plate are calculated according to equations (12) and (14). Fig. 2(b) and 2(c) show the contours of the time-invariant modal energy distribution $T_{11\_max} + V_{11\_max}$ and the Lagrangian density distribution $T_{11\_max} - V_{11\_max}$, respectively. It should be noted that the modal power flow is proportional to the gradient of the Lagrangian density distribution; hence, the modal power flow would be more sensitive to a disturbance to the plate than the modal energy distribution. Fig. 2(d) shows the vector field of the modal power flow $\vec{P}_{11}/D\omega_{11}$ of the intact plate. It is observed that power flow is smallest at the anti-nodes and the corners and power radiates in and out from the anti-nodes to the edges and the nodal line.

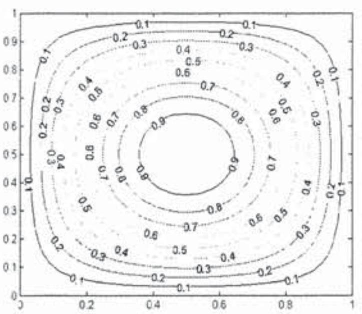

(a) Contours of vibration mode shape W_{11}

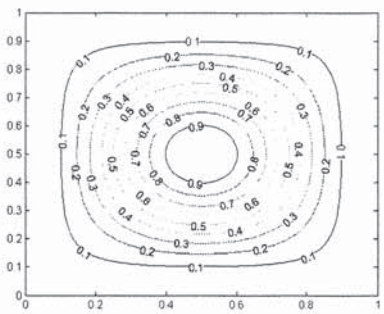

(b) Contours of the stationary modal energy ($T_{11\_max} + V_{11\_max}$).

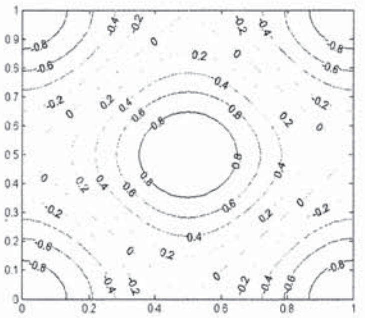

(c) Contours of the time varing modal energy ($T_{11\_max} - V_{11\_max}$).

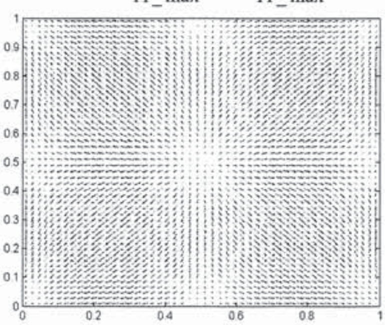

(d) Modal power flow $\vec{P}_{11}(x,y)/D\omega_{11}$ (illustrated by the arrows).

Fig. 2 Vibration mode shape, modal energies and modal power flow of a simply supported orthotropic composite plate.

3.2 Change of modal power flow in a damaged plate

Fig. 3(a) illustrates the presence of a region, $0.4 > x > 0.6$ and $0.4 > y > 0.6$, with stiffness reduction of 20% in the plate. Fig. 3(b) plots the contours of the first vibration mode shape of the damaged plate. Fig. 3(c) plots the contours of the first strain mode shape ε_{11_x} of the damaged plate. The damaged region cannot be identified based on the strain mode shape of the damaged plate. Fig. 3(d) and 3(e) show the time-invariant modal energy distribution $T_{11\_\max} + V_{11\_\max}$ and the Lagrangian density distribution $T_{11\_\max} - V_{11\_\max}$, respectively. It is observed that the modal energy distribution $T_{11\_\max} + V_{11\_\max}$ increases whilst the Lagrangian density distribution decreases in the damage region. These effects would be a result of the increase of strain energy in the damage region as pointed out in Section 2.3. Fig. 3(f) is a vector plot of the modal power flow in the damaged plate. Significant changes in amplitude and direction of the modal power flow can be observed in and around the damage region. These changes are consistent with the prediction as depicted by Eq. (26). Obviously, the modal power flow distribution is a local parameter sensitive to damage.

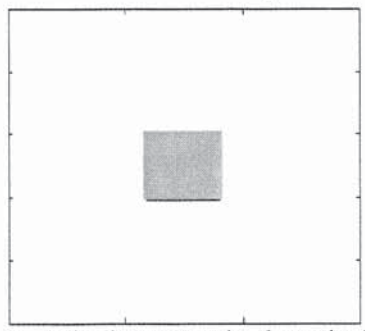

(a) A simply-supported orthotropic plate with a damaged (shaded) region of 20% *EI* reduction

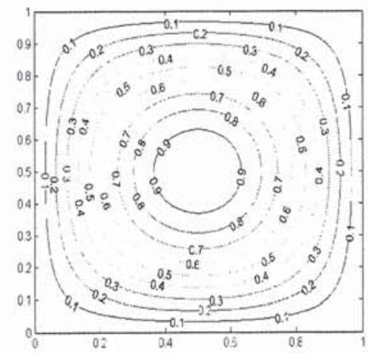

(b) Contours of vibration mode shape W_{11}

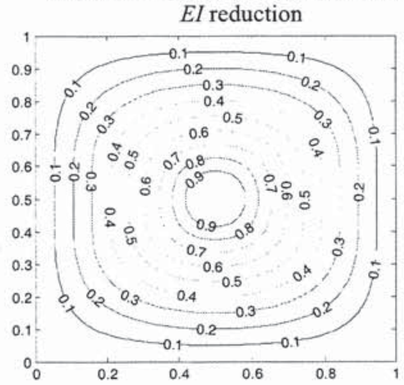

(c) Contours of the strain modeshape ε_{11_x} of the damaged plate.

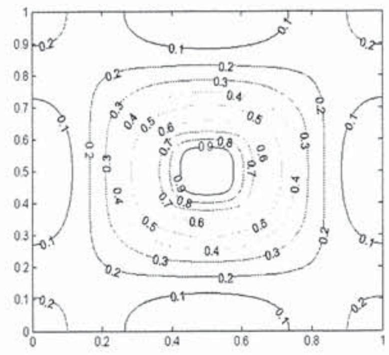

(d) Contours of the time varing modal energy ($T_{11\_\max} + V_{11\_\max}$).

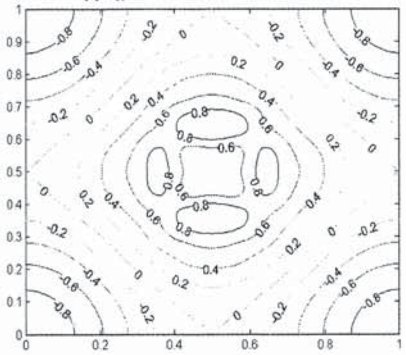

(e) Contours of the time varing modal energy ($T_{11\_\max} - V_{11\_\max}$).

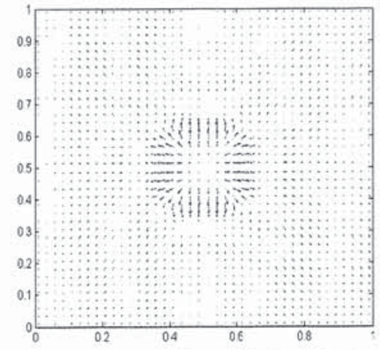

(f) Modal power flow $\vec{P}_{11}(x,y)/D\omega_{11}$ (illustrated by the arrows).

Fig. 3 Vibration mode shape, strain mode shape, modal energies and modal power flow of a damaged simply supported orthotropic composite plate.

4. Conclusions

Modal energy distributions and modal power flow in a damaged plate are studied, with the objective to demonstrate the capacity of modal power flow as a damage indicator. It is shown that the local time-averaged energy ($T_{max}+U_{max}$) increases at the damage region, hence the damage region behaves as an energy trap. Energy flowing in and out of the damage region to the surrounding regions may be increased or decreased depending on the location of the damage.

The capability for damage location identification for plate-like structures using modal reactive power flow is then demonstrated. Compared with the conventional damage indicators such as the change of strain mode shape of the plate, the proposed one is new and found to be more sensitive to the reduction of plate stiffness than the strain mode shape.

Moreover, compared with the damage identification techniques based on the determination of the active power flow in a damaged plate, the proposed method only requires information of a vibration mode shape of the structure and it is easier to apply in practice. Modal power flow of an orthotropic plate with a damaged region of reduced stiffness was analyzed. Numerical tests show that the modal power flow distribution is a local parameter sensitive to damage. Experimental study and validation will be carried out and reported in future.

References

(1) F.K. Chang, Structural health monitoring: current status and perspectives. Lancaster, Pennsylvania: Technomic publishing, 1997.

(2) A. Alvandi, C. Cremona, Assessment of vibration-based damage identification techniques. *Journal of Sound and Vibration* 292 (2006) 179-202.

(3) Y. Zou, L.Tong, G.P. Steven, Vibration-based model-dependent damage (delamination) identification and health monitoring for composite structures –a review. *Journal of Sound and Vibration* 230 (2000) 357-378.

(4) H.P. Chen, N.Bicanic, Asessment of damage in continuum structures based on incomplete modal information. *Computers and Structures* 74 (2000) 559-570.

(5) Y.Y. Li, L. Cheng, L.H. Yam and W.O. Wong, Identification of damage locations for plate-like structures using damage sensitive indices: strain modal approach, *Computers & Structures*, 80, (2002), 1881-1894.

(6) Z.Y. Shi, S.S. Law, L.M. Zhang, Structural damage localization from modal strain energy change, *Journal of Sound and Vibration* 218 (1998) 825-844.

(7) P. Cornwell, S.W. Doebling, C.R. Farrar, Application of the strain energy damage detection method to plate-like structures, *Journal of Sound and Vibration* 224 (1999) 359-374.

(8) N.K. Mandal, S. Biswas, Vibration power flow: a critical review, *The Shock and Vibration Digest* 37 (2005) 3-11.

(9) T.Y. Li, W.H. Zhang, T.G. Liu, Vibrational power flow analysis of damaged beam structures, *Journal of Sound and Vibration* 242 (2001) 59-68.

(10) M.S. Khun, H.P. Lee, S.P. Lim, Structural intensity in plates with multiple discrete and distributed spring-dashpot systems, *Journal of Sound and Vibration* 276 (2004) 627-648.

(11) H.P. Lee, S.P. Lim, M.S. Khun, Diversion of energy flow near crack tips of a vibrating plate using the structural intensity technique, *Journal of Sound and Vibration,* 296 (2006) 602-622.

(12) L. Gavric, G. Pavic, A finite element method for computation of structural intensity by the normal mode approach, *Journal of Sound and Vibration,* 164 (1993) 29-43.

(13) M.T. Whalen, The behavior of higher order mode shape derivatives in damaged, beam-like structures, *Journal of Sound and Vibration,* 309 (2008) 426-464.

(14) D.J. Ewins, *Modal testing : theory, practice and application*, Baldock, England: Research Studies Press, c2000.

(15) W.O. Wong, The effects of distributed mass loading on plate vibration behaviour, *Journal of Sound and Vibration*, 252 (2002) 577-583.

(16) Z.S. Liu, H.P. Lee, C. Lu, Structural intensity study of plates under low-velocity impact, *International Journal of Impact Engineering*, 31 (2005) 957-975.

(17) X.D. Xu, H.P. Lee, C. Lu, J.Y. Guo, Streamline representation for structural intensity fields, *Journal of Sound and Vibration,* 280 (2005) 449-454.

Acknowledgements

The authors wish to acknowledge support given to them by the Research Grants Council of The Hong Kong SAR Government through Grant No. PolyU 5340/09E.